



Journal of Advanced Research in Fluid Mechanics and Thermal Sciences

Journal homepage:
https://semarakilmu.com.my/journals/index.php/fluid_mechanics_thermal_sciences/index
ISSN: 2289-7879



Optimization of Process Economics in Mini Oil Refinery for Remote Areas

Rendra Panca Anugraha¹, Renanto Handogo^{1,*}, Ali Altway¹, Juwari Purwo Sutikno¹, Muhammad Fakhrizal Fahmi¹, Rizal Arifin¹, Vibianti Dwi Pratiwi¹

¹ Department of Chemical Engineering, Faculty of Industrial Technology and Systems Engineering, Institut Teknologi Sepuluh Nopember, Sukolilo, Surabaya 60111 Indonesia

ARTICLE INFO

Article history:

Received 25 June 2022

Received in revised form 22 November 2022

Accepted 1 December 2022

Available online 23 December 2022

Keywords:

Crude distillation; optimization; economic; mini refinery; Aspen Plus

ABSTRACT

The effects of the energy crisis and the rising energy demand have sparked development to improve efficiency in using fuel oil. According to Indonesia's oil resources, increasing refinery capacity and building mini refineries is essential to secure local refinery production. It is more effective and cost-effective to construct a small refinery with a configuration starting with a flash unit or pre-fractionator, to an atmospheric distillation unit, and a vacuum distillation unit as the last process in each oil-producing region than construct a large-scale refinery. The optimization concerned a variety of preflash furnace temperatures simulated by Aspen Plus software. The increasing temperature will change the production rate and the utility needed, which could change sales and operating costs. The result describes that the optimum profit for the mini-refinery plant is performed preflash furnace at 533 K with 108.20 US\$/m³ crude oil profit.

1. Introduction

Indonesia is the largest archipelagic country in the world and has the fourth largest population, with around 240 million people resulting in high energy needs. Indonesia has used fossil fuels, such as fuel oil, to meet domestic energy needs, as the primary energy source [1]. Indonesia has numerous renewable energy potentials. According to Lubis [2], who researched the energy equivalent potential of rice husk that was produced in 2015 created energy equivalent to 5 million kiloliters of gasoline. Lang *et al.*, [3] conducted a study on biogas upgrading plants to minimize reliance on fossil fuels, to reduce global warming. However, fossil resources in remote areas of Indonesia still need to be utilized, so a method to optimize these fossil fuels is required. Due to unfavorable geographic factors or the relatively low content of these sources, many oil and gas deposits in Indonesia have yet to be successfully used. Indonesia has sizable oil and gas reserves, amounting to 2.5 billion standard barrel tanks (Bsbt) and 50 trillion standard cubic feet of associated gas reserves (Tcf) [4]. In 2008, oil was the dominant energy source, with around 48% share of the energy mix, followed by coal at around 30% and natural gas at around 19% [5]. In 2019, the type of fuel for Indonesia's energy consumption

* Corresponding author.

E-mail address: renanto@chem-eng.its.ac.id

<https://doi.org/10.37934/arfmts.102.1.1424>

was the people's top choice, which accounts for 42% of energy consumption or the equivalent of 415.8 million barrels of oil. The impact of the energy crisis and high energy demand then encourage the development to increase fuel oil efficiency in terms of performance [6].

According to Indonesia's oil resources, increasing capacity and constructing new refineries are important to secure domestic refinery production. As anticipated, the Strategic Plan 2020–2024 for the Ministry of Energy and Mineral Resources outlines plans to improve domestic fuel output by expanding refinery capacity and looking into new refineries in Indonesia [7]. In 8 clusters in North Sumatra, Malacca Long Strait, Riau, Jambi, South Sumatra, South Kalimantan, North Kalimantan, and Maluku, the government intends to invest in micro refineries. Building these small refineries is anticipated to solve Indonesia's crude oil distribution and supply issues. In order to speed up the construction of oil refineries with a production capacity of 6,000–20,000 barrels per day, particularly in remote places, Handogo *et al.*, [8] study built a tiny oil refinery plant. One benefit of building a small refinery is that it takes less time to plan and build. Additionally, constructing small refineries in each oil-producing region is more effective and cost-effective than one massive refinery. Since oil from these regions must be transported to refineries, this can improve the economics of marginal fields [9].

Every day, refineries worldwide process thousands of barrels of crude oil to create different petroleum products. According to Zahid's [10] research, improving the efficiency of acid water units is the primary examination of the energy and economic factors in producing oil at refineries. Mini refineries perform more of a separation or refining process than large oil refineries, which contain complex operations up to the conversion phase. It is thought to be more profitable for small-scale oil refineries if the employed process is straightforward and does not demand high capital expenditures [8]. When developing a small oil refinery, the Vacuum Distillation Unit (VDU) and supporting fundamental processes are the main equipment. A preheat train, a flash unit or pre-fractionator, an atmospheric distillation unit, and a vacuum distillation unit are the typical components of crude oil distillation [11].

The high energy costs and ecological demands for high-quality oil products make optimizing the crude oil separation process more crucial. Refinery costs should be kept to a minimum—the prices of several pieces of furnace and heat exchanger equipment used in refineries to achieve design economy [8]. Crude oil will be heated to its maximum potential in the furnace at a temperature between 260°C and 300°C. The overall amount of product generated increases with increasing furnace temperature. However, the entire operation cost increases with furnace temperature [12]. In order to present a summary of the technical and economic features of the mini-oil refinery project, a preliminary study of the development plan is required.

2. Methodology

2.1 Process Description

In this study, the mini oil refinery uses Belida crude oil as a feed for 10,000 barrels/day or 1,607 m³/day. The specification of Belida crude oil has been explained entirely by Handogo *et al.*, [8]. Corrosion is unavoidable in petroleum refining, particularly in the crude unit. Corrosion monitoring is essential for controlling and predicting corrosion in chemical plant pipelines, vessels, furnace tubes, and other components [13]. The unit used for corrosion monitoring in crude oil refineries is Naphthenic Acid Corrosion (NAC) [14]. However, because Belida oil did not include any sulfides or other acids in this study, it did not affect the product. Meanwhile, the total acid number in Belida oil is below standard, around 0.057 mg KOH/g crude oil (based on the Ropital [15] study, TAN is 0.5 mg KOH/g crude oil). Therefore, naphthenic acid is not created in the product. Crude oil processing

includes three steps, preflash column, atmospheric distillation unit (ADU), and vacuum distillation unit (VDU) in Figure 1.

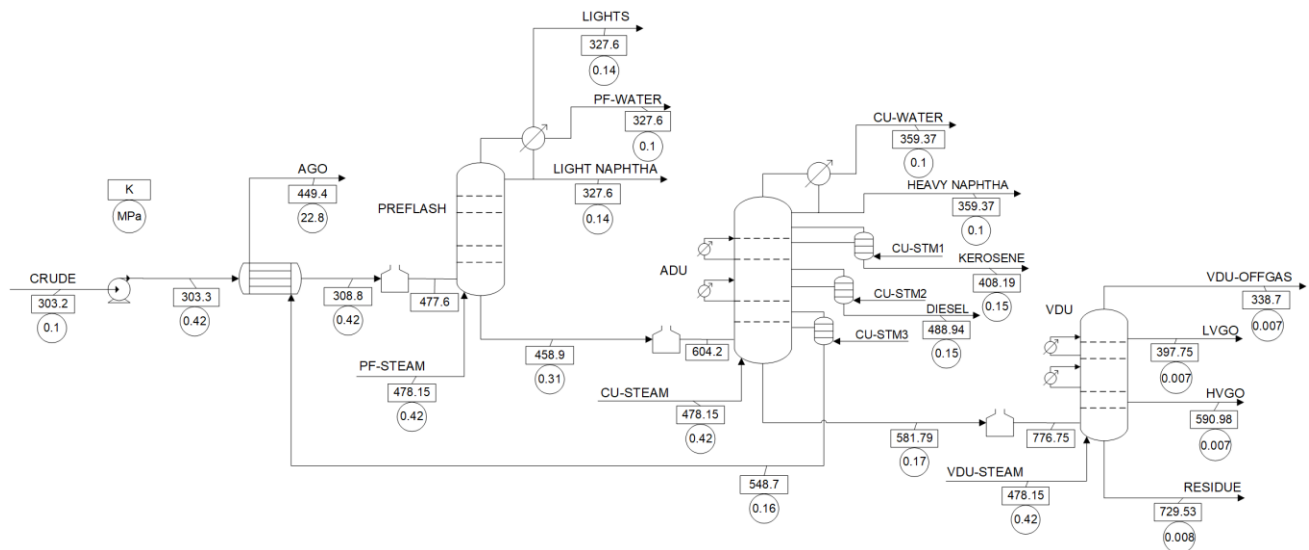


Fig. 1. Configuration of Mini Oil Refinery

The configuration in Figure 1 has been studied for its feasibility by Handogo *et al.*, [8]. However, several design specifications for unit operations, such as the tray number for each column, are relatively large for low-capacity of crude oil. Therefore, in this paper, design specifications are adapted from the Aspen Technology manual, which has a similar configuration but different specifications [16].

Pumping crude oil from storage into the furnace causes it to heat up to 308.8 K. Furnace working conditions are 477.6 K and 419.9 kPa, fed to a preflash column with ten stages. Open steam and crude oil are combined in the bottom stage preflash column, where the temperature is 478.15 K, and the pressure is 419.9 kPa. The top products from the preflash column, LIGHTS, and LIGHT NAPHTHA, were extracted using a partial condenser that ran at 327.6 K and 142.7 kPa. Design requirements for the product were LIGHT NAPHTHA with ASTM D86 95% at 405.4 K. The preflash column's bottom product passed into the ADU furnace and underwent additional vaporization, amounting to around 3% by volume. The ADU furnace's pressure was kept at 166.72 kPa. The theoretically 25-stage atmospheric distillation apparatus produced a complete condenser, three connected side strippers, and two pump-around circuits. If the stages are numbered from top to bottom, crude oil reaches the ADU on stage 22, which combines with the same open steam as in the preflash from the column's bottom stage. At various column sections, two pump-around were available to provide internal reflux. The pump-around has been located from stage 8 to stage 6 with a flow of 4900 barrels per day (779.04 m³/day) and a heat duty of -4.22 GJ/h. The second pump-around has been placed between stage 14 and stage 13, which has a heat duty of about -1.58 GJ/h and contains a flow of 1100 barrel/day or 174.89 m³/day, and the condenser has operated at atmospheric pressure.

The liquid drawn is located at stage 6 of the main column and the overhead return is located at stage 5 of the ADU column in the first side stripper. Output material in the stripper on the first side operating as KEROSENE. The three-stage second side stripper column connects at stage 13 as liquid draw and stage 12 as vapor return, and the output has been DIESEL product. Last, the third side column only has two equilibrium stages, producing an AGO stream with liquid feed entering stage 18 and outing vapor in stage 17. The top product of the ADU unit was HEAVY NAPHTHA-free water, and the bottom product flowed through to the vacuum distillation unit (VDU).

The furnace in the VDU unit has been set at 0.6% volume of fractional over-flash and 14 kPa of pressure. The last distillation column contains six equilibrium stages and obtains two pump-around. Additional open steam fed with crude from the furnace. The first pump-around has a functional specification of standard flow at 2000 barrels/day or 317.98 m³/day and heat duty at -1.55 GJ/h, the source stage in stage 2 and the destination stage in stage 1. The first pump-around produced LVGO. The second pump-around has a 4900 barrel/day or 779.04 m³/day flow and heat duty of -8.44 GJ/h at specification. The second pump is placed at draw stage 4 and returns to stage 3, producing HVGO. The top product of VDU is VDU-OFFGAS, and the bottom is RESIDUE.

2.2 Profit Calculation

The analysis of the process economics of a mini oil refinery employs profit optimization in the variation of a specific process parameter. In Handogo *et al.*, [12], the optimum profit is obtained by changing the furnace temperature in the preflash column. By adapting to their study, the profit calculation (P) is determined by total sales of oil products (S_{total}) subtracted from the refinery's operating cost (C_{op}) and formulated in Eq. (1).

$$P = S_{total} - C_{op} \quad (1)$$

The capital cost of the mini oil refinery is not included due to the assumption that the equipment size and design can accommodate the variation of the operating condition. To better understand the effect of the variation on the refinery's economics, each economic parameter is divided by the volume of the crude oil used (V_c).

The total product sales result from multiplying each product's price (S_p) by its amount (V_p) in kilograms and dividing by the volume of the crude oil, shown in Eq. (2). Table 1 provides each product's price, and the reference is based.

$$S_{total} = \frac{\sum_p S_p \times V_p}{V_c} \quad (2)$$

Table 1
 The price of each product and references

Products	Prices (US\$/1000 kg)	Reference
Light Naphtha	1186.00	[17]
Heavy Naphtha	1174.25	[18]
Kerosene	776.00	[19]
Diesel	1110.00	[20]
AGO	1080.00	[18]
VGO	763.50	[18]
Vacuum Residue	706.70	[21]

In this study, the operating cost consists of the cost of raw materials (C_c), the cost of steam (C_s), the cost of heat supply in furnaces (C_f), and the cost of cooling water (C_w), as shown in Eq. (3). The most recent data for the price of Belida crude oil is in 2021 data (C_c^{2021}), which is 438.02 US\$/m³. Therefore, the crude oil price estimation uses the ratio between the crude oil price in the 2021 (CCI_{2021}) and 2022 periods (CCI_{2022}), which is 458.34 US\$/m³ and 692.51 US\$/m³, respectively. Based on the description, the formulation is in Eq. (4).

$$C_{op} = C_C + C_S + C_F + C_W \quad (3)$$

$$C_C = C_C^{2021} \times \frac{CCI_{2022}}{CCI_{2021}} \quad (4)$$

As shown in Eq. (5), the cost of steam is calculated by using the cost index. The base price for steam is 2.75 US\$/1000 kg [21]. The cost index for industrial utilities in 2003 and 2022 is 100 and 209.149, denoted as (UCI_{2003}) and (UCI_{2022}) , respectively [23]. Notice the division with the volume of crude oil is present.

$$C_S = C_S^{2003} \times \frac{UCI_{2022}}{UCI_{2003}} \times \frac{1}{V_c} \quad (5)$$

Similarly, the cost index for industrial utilities is also used to calculate the cooling water price. The price of cooling water in 2003 was 0.08 US\$/1000 kg. The amount of cooling water is influenced by the heat duty (Q_C^{total}), the heat capacity of the water (cp_w), and the efficiency of heat transfer (η_c). For a typical cooling system, the temperature difference for cooling water (ΔT) is five centigrade, and the efficiency is 97%. Eq. (6) depicts the calculation of the cost of cooling water.

$$C_W = C_W^{2003} \times \frac{UCI_{2022}}{UCI_{2003}} \times \frac{Q_C^{total}}{\eta_c \times cp_w \times \Delta T} \times \frac{1}{V_c} \quad (6)$$

Natural gas is fuel for furnaces within the mini oil refinery, and the price is usually stated in energy units. The price for natural gas is 8.14 US\$/MMBtu [24]. In addition to the natural gas price (C_{NG}), the cost of heat supply in furnaces is also influenced by the total heat duty needed by furnaces (Q_F^{total}) and the furnace efficiency (η_F), as shown in Eq. (7).

$$C_F = C_{NG} \times \frac{Q_F^{total}}{\eta_F} \times \frac{1}{V_c} \quad (7)$$

3. Results and Discussion

Using the PetroFrac model, the performance optimization was carried out in Aspen Plus software [16]. As the first step, steady-state simulation was done with a furnace temperature of 477.6 K. In setting up the simulation of the distillation process, assigning an appropriate fluid package is critical to accurately describe the phase equilibrium inside the column [25]. The typical suitable method for the oil refining process can be divided into two groups. The use of the state equation of gasses defines the first group, which includes The Peng-Robinson (PR) dan Soave Redlich Kwong (SRK). The second group is developed for specific usage in hydrocarbon mixtures and is suitable mainly for predicting the properties of pseudo components. Chao-Seader and Braun K10 is an example of this model [26]. Preliminary analysis from the base case simulation results in a slight deviation in product yield when using Chao-Seader, PR, and SRK. Moreover, the Braun K10 generate accurate result compared to the reference [16]. Therefore, the Braun K10 is used as the thermodynamic method in this study.

The selection of operating parameters as a variable depends on the influence of the parameter on the product flowrate. As the first column in the configuration, the Preflash column will impact the

overall operation. In theory, four operating parameters in the preflash column influence the overall process, which includes column pressure, reflux-drum temperature, furnace temperature, and the number of stages. In Luyben [25], these parameters have been studied for their effect on the yield product of light and heavy naphtha. However, the other products are yet to be studied the effect. In the study by Handogo *et al.*, [12], the change in preflash column furnace temperature affects the phase equilibrium and product flowrate in the preflash and pipestill columns. Therefore, the temperature of the preflash furnace is chosen as the variable to optimize refinery profit.

The increasing vaporization rate in the furnace due to increased temperature led to rising heat duty in the preflash furnace, as shown in Table 2. More vaporization rate also affects the reflux rate and heat duty of the condenser in the preflash column, which is explained by the vapor-liquid equilibrium of the column. More vapor flow leads to more mass load into the top column, increasing the cooling duty required to separate the vapor and liquid phase in the reflux drum. Consequently, the cooling duty in the condenser is increasing. In addition, more vapor flow also increases the number of heavier fractions in the top column, in which not all components are desired to produce a specified light naphtha. However, after the condenser's cooling process, the stream's low temperature can be utilized to balance the vapor-liquid equilibrium in the column. Hence, some of the subcooled liquid is recycled back into the column, leading to an increasing reflux ratio.

Table 2
 Steady-state simulation results in operating condition

	Preflash column furnace temperature (K)				
	478	505	533	561	589
Reflux ratio preflash	1.06	1.66	2.42	3.29	4.21
Reflux ratio ADU	3.57	4.35	4.88	5.20	5.39
Heat duty furnace preflash (GJ/h)	17.98	23.00	28.30	33.63	38.89
Heat duty furnace ADU (GJ/h)	27.64	24.15	21.72	20.17	19.23
Heat duty furnace VDU (GJ/h)	9.77	9.68	9.62	9.59	9.58
Heat duty condenser preflash (GJ/h)	-10.67	-14.50	-18.74	-23.27	-27.99
Heat duty condenser ADU (GJ/h)	-21.54	-20.52	-20.04	-19.81	-19.68

The increasing temperature furnace of the preflash column also affects operation in subsequent columns, ADU and VDU. In Table 3, more product is obtained at the top column of the preflash. As a result, the bottom product of the preflash column, which is a feed to the following process, decreases. The less mass load to the column will reduce the energy required in the furnace of ADU and VDU. The correlation can also be applied to the decreasing energy required in the condenser of ADU. As shown in Table 3, the increasing preflash column temperature improves the amount of light naphtha produced but reduces the flowrate of heavy naphtha. This is caused by some naphtha that initially should be obtained as heavy naphtha is partially vaporized in the preflash column. Contrary to the study by Luyben [25], other products, such as Kerosene, Diesel, AGO, VGO, and Vacuum Residue, show an apparent change in their production rate. However, the change in product yield is less significant than light and heavy naphtha.

Table 3
 Mass balance and yield product of the optimization

		Preflash column furnace temperature (K)				
		478	505	533	561	589
1	Feed mass flowrate (kg/h)					
-	Crude oil	52300	52300	52300	52300	52300
-	Steam Preflash	1478	1478	1478	1478	1478
-	Steam ADU	2710	2710	2710	2710	2710
-	Steam VDU	500	500	500	500	500
	Total feed mass flowrate (kg/h)	56988	56988	56988	56988	56988
2	Product mass flowrate (kg/h)					
-	Off-Gas PF	273	121	54	23	8
-	Light Naphtha	7325	8561	9143	9424	9574
-	Heavy Naphtha	7780	6324	5620	5273	5086
-	Kerosene	5866	5855	5849	5846	5844
-	Diesel	13494	13917	14133	14242	14301
-	AGO	4711	4712	4713	4713	4713
-	Off-Gas VDU	500	500	500	500	500
-	LVGO	2318	2280	2261	2251	2246
-	HVGO	8932	8933	8933	8933	8933
-	Vacuum Residue	1650	1641	1636	1634	1633
-	Water	4140	4145	4147	4148	4148
	Total product mass flowrate (kg/h)	56988	56988	56988	56988	56988

The result of the calculation of the economic parameters is presented in Table 4 and Table 5. Table 4 displays the sales of each product in different preflash furnace temperatures. Even though the price of diesel products is not the highest, high-yield production cause diesel generates the highest revenue. Figure 2, which illustrates the result in Table 4, shows that light and heavy naphtha are the most significant change compared to the other products. The change is also consistent with increasing or decreasing the product flowrate. Moreover, total sales, which are illustrated in Figure 3, are continuously increasing and have yet to reach the extreme point. However, the total product rises steeply at a range temperature of 478 – 505 K and slows at a higher range.

Table 4
 Sales of each product in different preflash furnace temperature

Product	Preflash column furnace temperature (K)				
	478	505	533	561	589
	Product sales (US\$/m ³ crude oil)				
Light Naphtha	131.14	153.28	163.68	168.73	171.40
Heavy Naphtha	137.90	112.10	99.61	93.46	90.16
Kerosene	68.72	68.58	68.51	68.48	68.46
Diesel	226.10	233.19	236.81	238.64	239.63
AGO	76.81	76.83	76.83	76.84	76.84
VGO	129.65	129.23	129.02	128.91	128.85
Vacuum Residue	17.60	17.51	17.46	17.44	17.42
Total product sales	787.92	790.70	791.93	792.48	792.77

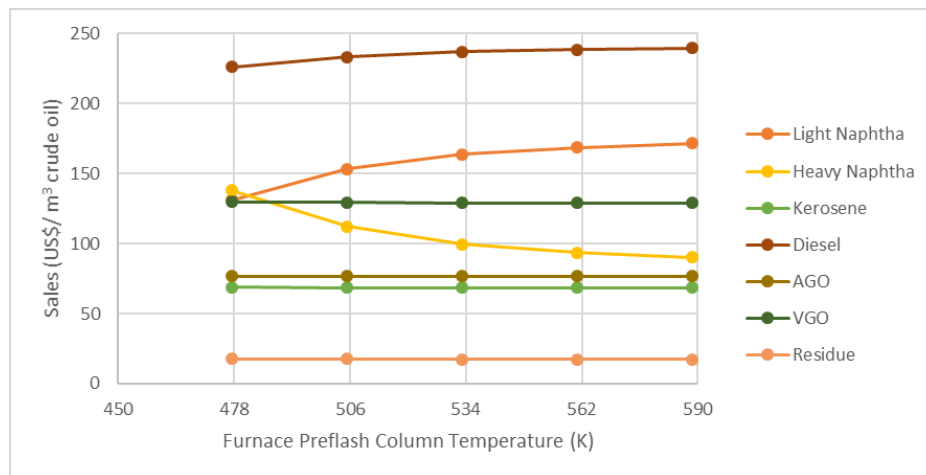


Fig. 2. Effect of preflash column furnace temperature on sales of each product

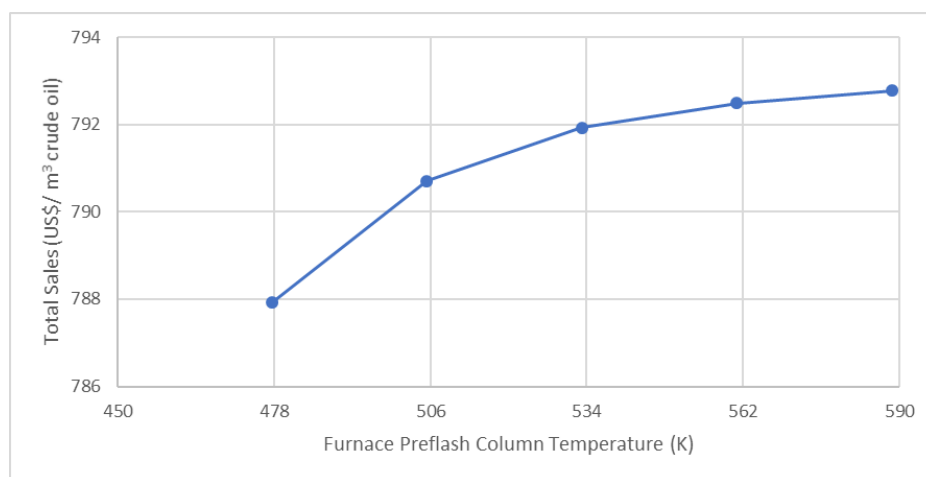


Fig. 3. Effect of preflash column furnace temperature on total sales

The result of the calculation of operation cost and its component is tabulated in Table 5. Most of the operation cost is expended on crude oil as raw material. The cost of steam is constant due to the value staying constant in different preflash furnace temperatures as opposed to the cost of cooling water and heat supply for the furnace. The total cooling water cost is based on the sum of every condenser's heat duty. In the previous study, the cooling water cost is neglected due to its price being insignificant compared to the cost of steam, where the ratio between the price of cooling water and steam is 1:55 [12]. However, the cooling water cost calculation depends not only on its price but also includes the amount of water used. The amount of both utilities can be seen in Table 6. The ratio of water used and steam required reaches over 1000:1 at high temperatures. Even though the small price of the cooling water is, the calculated mass load demands a huge amount of water. Therefore, it is required to include cooling water in the operation cost. The total cost of cooling water and heat supply for the furnace shows a steady increase in Figure 4.

Table 5
 Result of operation cost and profit calculation

	Preflash column furnace temperature (K)				
	478	505	533	561	589
Total product sales (US\$/m ³ crude oil)	787.92	790.70	791.93	792.48	792.77
Cost of raw material (US\$/m ³ crude oil)	661.81	661.81	661.81	661.81	661.81
Cost of steam (US\$/m ³ crude oil)	6.11	6.11	6.11	6.11	6.11
Total cost of cooling water (US\$/m ³ crude oil)	5.79	6.12	6.57	7.09	7.65
Total cost of heat supply in furnaces (US\$/m ³ crude oil)	8.27	8.68	9.23	9.86	10.53
Total operation cost (US\$/m ³ crude oil)	681.98	682.73	683.73	684.87	686.10
Profit (US\$/m ³ crude oil)	105.93	107.97	108.20	107.61	106.67

Unlike the total sales, operation costs rapidly increase in the higher temperature range. This is influenced by the more significant number of utilities required when the preflash furnace temperature is higher. The rapid increase in the operation cost allows for determining the optimum point from profit correlation to the preflash furnace temperature, as illustrated in Figure 5. The explanation of Figure 5 is as follows; Profit is described using the right side of the y-axis, and total sales and operation costs are shown on the left side of the y-axis. The profit grows fast in low-range temperatures, and as the temperature increases, the operational cost ramps up, the profit starts to flatten, and then the profit decreases. Therefore, the optimum profit can be determined at the maximum extreme point of the graph. As shown in Figure 5, the maximum profit is at 108.20 US\$/m³ crude oil when the preflash furnace temperature is 533 K.

Table 6
 Utility usage in different preflash furnace temperature

	Preflash column furnace temperature (K)				
	478	505	533	561	589
Total steam (kg/h)	2,933	2,933	2,933	2,933	2,933
Total cooling water (kg/h)	2,290,984	2,424,414	2,603,161	2,808,091	3,027,119
Total heat natural gas (MMBtu/h)	52.50	53.86	56.53	60.09	64.16

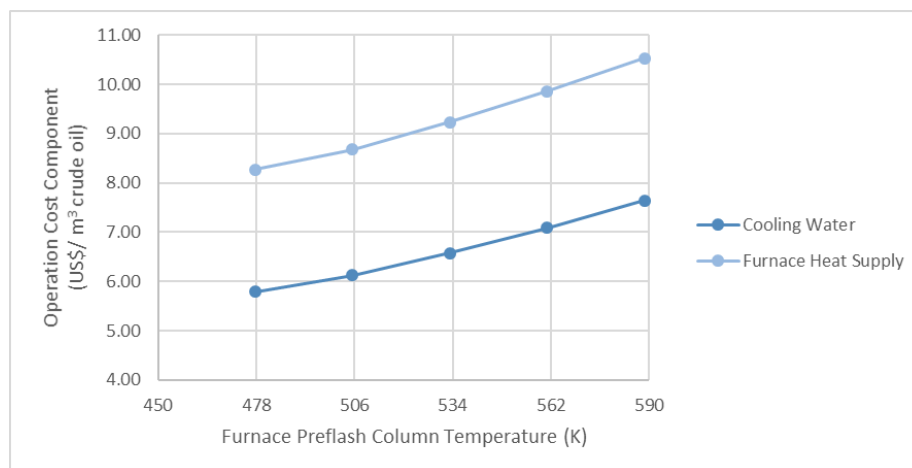


Fig. 4. Effect of preflash column furnace temperature on the total cost of cooling water and furnace heat supply

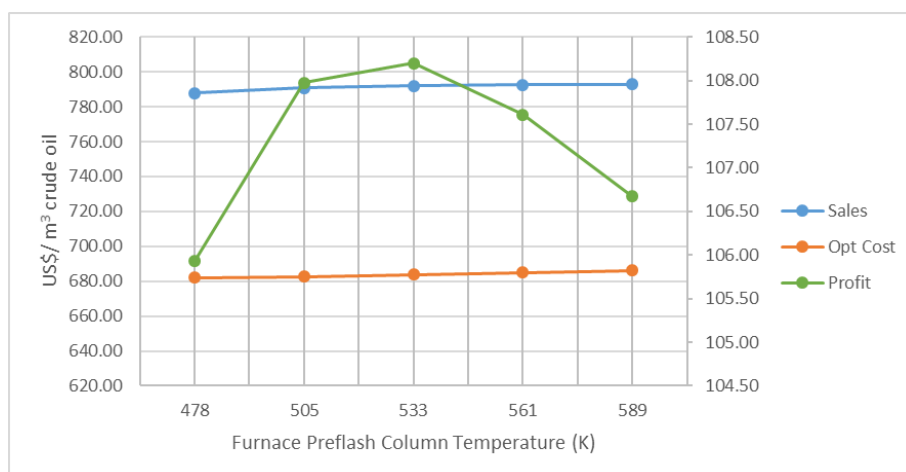


Fig. 5. Effect of preflash column furnace temperature on the total sales, total operating cost, and profit

4. Conclusions

Based on the study, it can be concluded that a Mini Oil Refinery Plant has an optimum profit of 108.20 US\$/m³ crude oil when the preflash furnace temperature is at 533 K. The maximum profit in a different range of preflash furnace temperature determines the optimum point. The change in preflash furnace temperature impacts not only the production rate of naphthas but also affects yield for every product. However, the effect is more significant in light and heavy naphtha. In addition, the varied temperature also affects important operating conditions, changing the operational cost.

Acknowledgement

This work was supported by KEMENDIKBUDRISTEK under the “Hibah Penelitian Dasar Unggulan Perguruan Tinggi” (PDUPT) number: 008/E5/PG.02.00.PT/2022 and DRPM Institut Teknologi Sepuluh Nopember number: 1548/PKS/ITS/2022.

References

- [1] Anugraha, Rendra Panca, Rifky Arya Maulana, and Rasyid Dito Kusumo. "Cost And Product Optimization of Upgrading Light Naphtha Using Pressure Swing Adsorption Method by Aspen Adsorption Simulation." *Journal of Advanced Research in Fluid Mechanics and Thermal Sciences* 100, no. 2 (2022): 198-210. <https://doi.org/10.37934/arfmts.100.2.198210>
- [2] Lubis, Hamzah. "Renewable Energy of Rice Husk for Reducing Fossil Energy in Indonesia." *Journal of Advanced Research in Applied Sciences and Engineering Technology* 11, no. 1 (2018): 17-22.
- [3] Lang, Kwong Cheng, Lian See Tan, Jully Tan, Azmi Mohd Shariff, and Hairul Nazirah Abdul Halim. "Life cycle assessment of potassium lysinate for biogas upgrading." *Progress in Energy and Environment* 22 (2022): 29-39. <https://doi.org/10.37934/progee.22.1.2939>
- [4] Ministry of Energy and Mineral Resources, (2018). *Handbook of Energy and Economic Statistics of Indonesia 2018*.
- [5] Stünkel, S., A. Drescher, J. Wind, T. Brinkmann, J-U. Repke, and G. Wozny. "Carbon dioxide capture for the oxidative coupling of methane process—A case study in mini-plant scale." *Chemical Engineering Research and Design* 89, no. 8 (2011): 1261-1270. <https://doi.org/10.1016/j.cherd.2011.02.024>
- [6] Speight, James G. *Handbook of industrial hydrocarbon processes*. Gulf Professional Publishing, 2019.
- [7] Ministry of Energy and Mineral Resources, (2020). *Peraturan Menteri Energi dan Sumber Daya Mineral Republik Indonesia Nomor 16 Tahun 2020 Tentang Rencana Strategis Kementerian Energi Dan Sumber Daya Mineral Tahun 2022-2024*.
- [8] Handogo, Renanto, Fery Prasetyo, Santi Puspita Sanjaya, and Rendra Panca Anugraha. "Preliminary Design of Mini Oil Refinery Plant." *Journal of Advanced Research in Fluid Mechanics and Thermal Sciences* 92, no. 1 (2022): 39-50. <https://doi.org/10.37934/arfmts.92.1.3950>

- [9] Chabibulloh, Bilal, Wisnu Kusuma Atmaja, Juwari Purwo Sutikno, and Renanto Handogo. "Pra Desain Pabrik Produksi Gasoline pada Kilang Minyak Skala Kecil." *Jurnal Teknik ITS* 7, no. 1 (2018): F127-F131. <https://doi.org/10.12962/j23373539.v7i1.28915>
- [10] Zahid, Umer. "Techno-economic evaluation and design development of sour water stripping system in the refineries." *Journal of Cleaner Production* 236 (2019): 117633. <https://doi.org/10.1016/j.jclepro.2019.117633>
- [11] Wang, Ziyuan, Qiang Xu, and Thomas Ho. "Optimal retrofit design of crude distillation units for processing shale gas/natural gas condensate oil." *Chemical Engineering & Technology* 39, no. 6 (2016): 1099-1110. <https://doi.org/10.1002/ceat.201500227>
- [12] Handogo, Renanto. "Optimization on the performance of crude distillation unit (CDU)." *Asia-Pacific Journal of Chemical Engineering* 7 (2012): S78-S87. <https://doi.org/10.1002/apj.644>
- [13] Schempp, Philipp, Karsten Preuß, and Micha Tröger. "About the correlation between crude oil corrosiveness and results from corrosion monitoring in an oil refinery." *Corrosion* 72, no. 6 (2016): 843-855. <https://doi.org/10.5006/1940>
- [14] Subramanian, Chidambaram. "Corrosion prevention of crude and vacuum distillation column overheads in a petroleum refinery: A field monitoring study." *Process Safety Progress* 40, no. 2 (2021): e12213. <https://doi.org/10.1002/prs.12213>
- [15] Ropital, F. "Environmental degradation in hydrocarbon fuel processing plant: issues and mitigation." In *Advances in Clean Hydrocarbon Fuel Processing*, pp. 437-462. Woodhead Publishing, 2011. <https://doi.org/10.1533/9780857093783.5.437>
- [16] Aspen Technology Inc. "Getting Started: Modeling Petroleum Processes." (2006).
- [17] Chemanalyst. Naphtha Price Trend and Forecast.
- [18] S&P Global Commodity Insight, 2022. Platts Asia-Pacific/Persian Gulf Market 41 (83).
- [19] Chemanalyst. Jet Kerosene Price Trend and Forecast.
- [20] Chemanalyst. Diesel Price Trend and Forecast.
- [21] Maryland Asphalt Association. Asphalt Index.
- [22] Peters, Max Stone, Klaus D. Timmerhaus, and Ronald Emmett West. *Plant design and economics for chemical engineers*. Vol. 4. New York: McGraw-hill, 2003.
- [23] U.S Bureau of Labor Statistics. Producer Price Index - Utilities. Accessed December 16, 2022.
- [24] U.S Energy Information Administration. Natural Gas Prices. Accessed December 16, 2022.
- [25] Luyben, William L. *Distillation design and control using Aspen simulation*. John Wiley & Sons, 2013. <https://doi.org/10.1002/9781118510193>
- [26] Haydary, Juma, and Tomáš Pavlík. "Steady-state and dynamic simulation of crude oil distillation using Aspen Plus and Aspen Dynamics." *Petroleum & coal* 51, no. 2 (2009): 100-109.